A Letters Journal Exploring the Frontiers of Physics

August 2017

EPL, **119** (2017) 30004
doi: 10.1209/0295-5075/119/30004

www.epljournal.org

Reconstruction of a scalar voltage-based neural field network from observed time series

A. Pikovsky

Institute for Physics and Astronomy, University of Potsdam - Karl-Liebknecht-Str. 24/25, 14476 Potsdam-Golm, Germany and
Research Institute for Supercomputing, Nizhni Novgorod State University - Gagarin Av. 23, 606950 Nizhni Novgorod, Russia

received 22 August 2017; accepted in final form 24 September 2017
published online 24 October 2017

PACS 05.45.Tp – Time series analysis
PACS 87.19.lj – Neuronal network dynamics
PACS 05.45.Jn – High-dimensional chaos

Abstract – We present a general method for the reconstruction of a network of nonlinearly coupled neural fields from observations. A prominent example of such a system is a dynamical random neural network model studied by Sompolinsky *et al.* (*Phys. Rev. Lett.*, **61** (1988) 259). We develop a technique for inferring the properties of the system from the observations of the chaotic voltages. Only the structure of the model is assumed to be known, while the nonlinear gain functions of the interactions, the matrix of the coupling constants, and the time constants of the local dynamics are reconstructed from the time series.

Introduction. – Reconstruction of networks based on the observation of their dynamics is a challenging problem relevant for many interdisciplinary applications in physics, climate system analysis, biochemical and biological dynamics, genetic regulation, epidemiology [1–7] and even in social sciences [8]. Particularly broad are applications in neurosciences, aimed at an understanding of brain connectivity and functionality [9–13]. Here one tries to reconstruct the interactions between the nodes exploring multivariate neurophysiological measurements [14–16].

Generally, methods of reconstruction can be divided in two classes. In the first approach, one explores statistical interdependencies of observed stochastic processes, and calculates cross-correlations and mutual (Granger) information measures [17–20]. In another class of methods, one assumes a complex dynamical system behind the observations, and tries to reconstruct the network on the basis of the deterministic dynamics [21–26].

Here we propose a dynamics-based method for reconstruction of a neuronal network from the observed voltages of the nodes. We assume that the dynamics is governed by a generic system of coupled neural fields, where all the elements —the gain functions, the time constants, and the coupling constants of the interaction— are unknown. In the course of the reconstructions, based on the multivariate time series of voltages, these parameters and functions are inferred.

Neural network model and its dynamics. – In this paper we focus on the reconstruction of the network structure that governs neural fields in the voltage formulation, one of the basic models in computational neuroscience (see refs. [27–29]). Each of the n nodes is characterized by its time-depending voltage $x_j(t)$, the evolution of which is governed by the inputs from other nodes according to a system of ordinary differential equations

$$\frac{\mathrm{d}x_j}{\mathrm{d}t} + \gamma_j x_j = \sum_{k=1}^{n} C_{jk} F_k(x_k), \quad j = 1, \ldots, n. \qquad (1)$$

Here γ_j is the time constant of relaxation of the field at node j, and F_k are the gain functions at the nodes (typically $F(x) \sim \tanh(x)$ or have some similar form). The network is determined by the $n \times n$ coupling matrix C_{jk}. As has been shown in ref. [30], at strong enough coupling such a network demonstrates chaos, and this is a state which allows the reconstruction of the network matrix C_{jk}, the time constants γ_j, and the functions F_k from the set of observations $x_j(t)$, as described below (see "Conclusions" for a possible extension to non-chaotic states).

For our approach the most important property of the model (1) is its scalar character: the dynamics at each

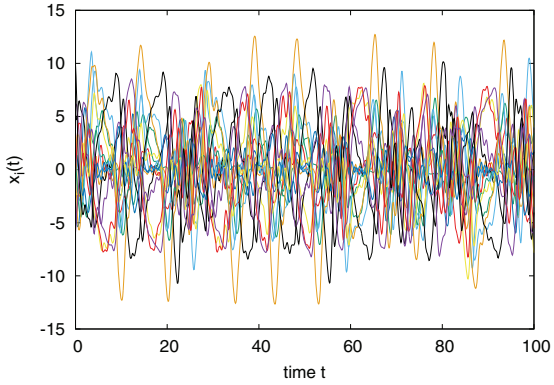

Fig. 1: (Color online) Example of chaotic neural fields $x_i(t)$ in model (1).

node is one dimensional, so it is fully characterized by a scalar variable x_k, and the nonlinear function F is a function of one variable. This should be contrasted to more general networks where the dynamics at each node is high dimensional.

First, we illustrate a chaotic state in system (1). To be as close as possible to the theoretical approach of ref. [30], we take $F(x) = \tanh(x)$ and choose C_{ij} to be independent random variables with a Gaussian distribution with zero mean and standard deviation 2 (the standard deviation is an essential parameter in theory [30], chaos in a network is typically observed for large enough values of this parameter). The time constants γ_j are chosen from a uniform distribution in the range $0.8 < \gamma < 1.2$. An example of a chaotic regime for an ensemble of $N = 16$ elements is presented in fig. 1. The calculated largest Lyapunov exponent is 0.22. This chaotic state is used below in all calculations for the illustration of the reconstruction method.

Reconstruction of the network parameters. –

Method of the reconstruction: known time constants. Here we present the method of the reconstruction, assuming that the time constants γ_j are known. We will extend to the case of unknown constants γ_j in the next subsection.

Suppose one observes the time series of all variables $x_j(t)$ governed by eq. (1). The problem is to reconstruct the coupling matrix C and the functions F_k from these observations. First, we calculate the time derivatives of the observed signals to obtain the time series $(\dot{x}_j, x_j)$. Let us invert eqs. (1):

$$F_j(x_j) = \sum_i W_{ji}(\dot{x}_i + \gamma_i x_i). \qquad (2)$$

Here $W = C^{-1}$ is the matrix inverse to the coupling matrix C. This matrix generally exists, as the random matrix C is typically non-singular.

The main idea of the reconstruction follows from the functional relation of the scalar variable x_j and the r.h.s. of eq. (2). For the sake of simplicity of presentation we denote $y_i(t) = \dot{x}_i + \gamma_i x_i$. Suppose that in the chaotic time series $x_j(t)$, we find two time instants, t_1 and t_2, such that $x_j(t_1) \approx x_j(t_2)$. Then, from eq. (2) it follows that $\sum_i W_{ji} y_i(t_1) \approx \sum_i W_{ji} y_i(t_2)$. Here, in fact, only the continuity of the function F_j is used; no other assumptions are needed. This relation can be rewritten as

$$\sum_i W_{ji} z_i \approx 0, \qquad z_i = y_i(t_1) - y_i(t_2). \qquad (3)$$

We expect that for a chaotic time series this relation is nontrivial, *i.e.* the vector z_i does not vanish. (For a periodic time series one can obviously find such points that $y_i(t_2) \approx y_i(t_1)$, if $t_2 - t_1$ is a multiple of the period. As discussed in "Conclusions" below, only periodic regimes with a complex waveform may provide enough nontrivial recurrent points to ensure reconstruction.)

For a sufficiently long scalar time series $x_j(t)$, we in fact can find many such time instants where $x_j(t_1) \approx x_j(t_2)$, and correspondingly we have a large set of M vectors $z_i{}^{(m)}$, $m = 1, \ldots, M$. The size of the set M is the essential parameter of the method, as dicussed below it is close to the length of the observed time series. Using a vector notation $\{z_i^{(m)}\} = \vec{z}^{(m)}$, we thus obtain a set of equations

$$\vec{w}_j \cdot \vec{z}^{(m)} = 0, \qquad (4)$$

where we denoted the j's row of the matrix W as a vector: $[\vec{w}_j]_i = W_{ji}$.

The problem of finding the vector $\vec{w}_j$ from the set of linear equations (4) is the standard problem of finding a null space of the $N \times M$ matrix composed of M vectors $\vec{z}^{(m)}$. This problem can be straightforwardly solved via Singular Value Decomposition (SVD) [31]. Once the zero singular value is found, the corresponding entry in the obtained unitary matrix gives the vector $\vec{w}_j$. Performing this for different rows j allows us to obtain the matrix W. We note that the matrix is obtained unambiguously up to a normalization, because the functions F_j in (2) are unknown. If one assumes these functions to be normalized, then the inverse coupling matrix W is defined in a unique way. Together with the time series $y_i(t)$, this matrix defines according to eq. (2) the gain functions F_j. Finally, the coupling matrix C is obtained by the inversion of W (we remind that the time constants γ_j are assumed to be known in this variant of the method). Practically, one obtains not exact null spaces, but spaces corresponding to the minimal singular values $S_j^{(min)}$, which are small but do not vanish exactly.

In the procedure above we have to find close returns of the time series $x_j(t)$. Because this time series is a scalar one, the following simple technique could be used. One just performs a sorting of the available array of values x_j. Then the neighboring values of x_j in the sorted array (although they are of course typically not neighbors in the original time series if the sampling rate is not too large; for a large sampling rate one needs to exclude neighbors within, say, a typical correlation time in the original time series) provide the closest returns. If the range of values of

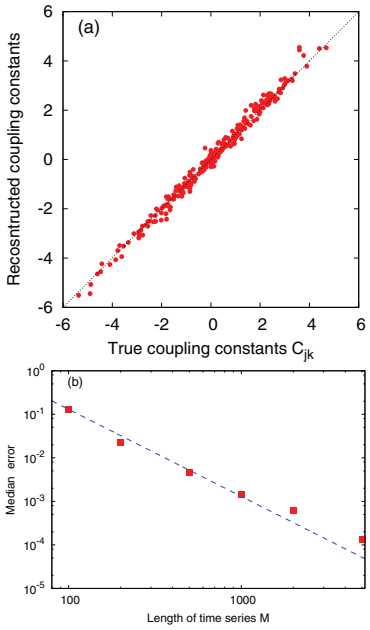

Fig. 2: (Color online) Reconstruction of the coupling constants. Time derivatives are calculated via the Savitzky-Golay filter with parameters [6,6], for the time step $\mathrm{d}t = 0.01$. Points for the analysis were taken with step $\Delta t = 2$. Panel (a): reconstructed *vs.* true coupling constants for $M = 100$. The dotted line is the diagonal. Panel (b): dependence of the median error on the length of the time series M (square markers). The dashed line has slope of -2.

x is Δ, then for M points in the chaotic time series one can estimate $|x_j - \hat{x}_j| \sim \Delta/M$, where $\hat{x}_j$ is a close neighbor of x_j after sorting. One can see that the error vanishes for a very long time series $M \to \infty$. Furthermore, taking only nearest neighbors in the sorted time series, one avoids redundancy in the matrix of vectors $\vec{z}^{(m)}$, as each value of x_j participates only twice in the formation of the set of $\vec{z}^{(m)}$.

We illustrate the method in fig. 2. Here we used a multivariate time series $x_j(t)$ depicted in fig. 1, from which the time derivatives have been calculated by virtue of the Savitzky-Golay filter. Panel (a) shows the reconstructed coupling constans of the matrix C *vs.* the original ones, for a rather small length of the time series $M = 100$. Panel (b) shows the dependence of the median error on the length of the time series M (we use median because of a broad distribution of errors, cf. fig. 3(b) below). This dependence fits quite well the scaling $Err \sim M^{-2}$.

To check the robustness of the method to different levels of noise in the data, we performed the same analysis as shown in fig. 2 for the time series with added observational Gaussian noise with standard deviation σ. Partially this noise is filtered out due to application of the Savitzky-Golay filters needed also to calculate the time derivatives. Figure 3 illustrates the quality of the reconstruction for four different values of σ. One can see that the errors are proportional to the noise level. The reconstruction is, nevertheless, quite robust as even for a large noise level

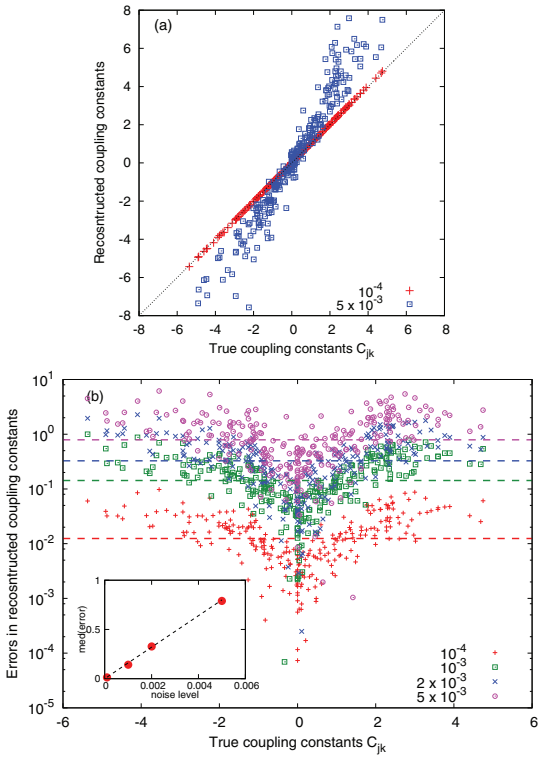

Fig. 3: (Color online) Reconstruction of coupling constants in the presence of noise. Time derivatives are calculated via the Savtzky-Golay filter with parameters [6,6], for the time step $\mathrm{d}t = 0.01$. Points for the analysis were taken with step $\Delta t = 2$, the total number of points was $M = 1000$. Four levels of noise have been explored. Panel (a) shows the reconstructed *vs.* true coupling constants for $\sigma = 10^{-4}$ (pluses, nearly perfect reconstruction for the minimal noise level) and $\sigma = 5 \cdot 10^{-3}$ (squares, rather large level of errors). The dotted line is the diagonal. Panel (b) shows all the errors in the reconstructed coupling constants *vs.* the true ones, for four indicated levels of noise. Dashed lines show the medians of these errors. The inset in panel (b) depicts the linear dependence of the median of the errors *vs.* noise level (the dashed straight line has slope 160).

in fig. 3(a), the reconstructed coupling constants though inaccurate in absolute values, are nevertheless roughly linearly proportional to the true values (cf. squares in fig. 3(a)) and this allows distinguishing strong and weak links in the network.

Unknown time constants. Above we have assumed that the time constants γ_j at the nodes are known. This allowed us to calculate the values $y_i(t)$ explicitely. In the case of unknown γ_j this is not possible, and to apply the method above we have to scan over different test values of γ_j. An indicator for the correct choice of the time constants is the quality of the found null space of the system of eq. (4). Practically, we used the maximum over the index j singular value

$$S(\vec{\gamma}) = \max_j S_j^{(min)} \tag{5}$$

as the cost function, trying to minimize it.

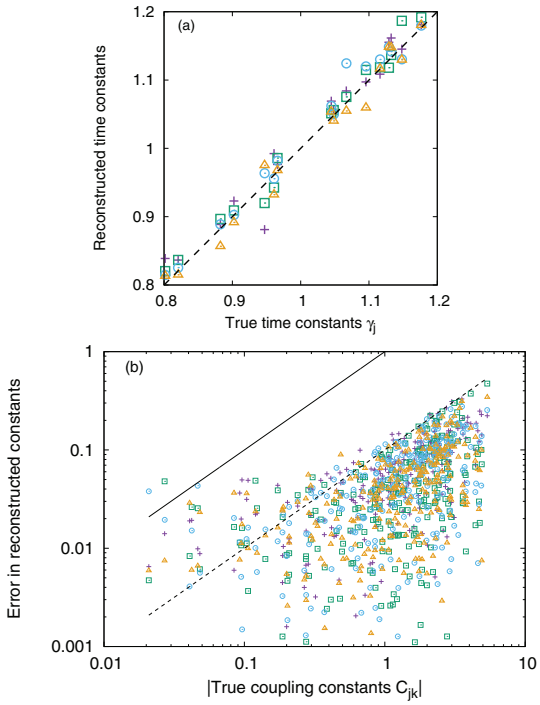

Fig. 4: (Color online) Reconstructed time constants (a) and the error $Er = |C_{rec,jk} - C_{jk}|$ in the reconstructed coupling constants *vs.* the true constants themselves (b). Four symbols show four independent runs of the simulated annealing routine. Number of points used $M = 1000$. In panel (b) the two lines show the levels $Er = C$ (solid line) and $Er = 0.1C$ (dashed line). As most of the values lie below the dashed line, the maximal error of the method can be estimated as 10%, except for coupling constants that are very small —for them the relative error is of order 1.

Unfortunately, in the definition of vectors y_i and $\vec{z}^{(m)}$ all the time constants enter, so one has to scan in the full N-dimensional space to find an absolute minimum of $S(\vec{\gamma})$. Thus, because a brute force approach is hardly possible, a more sophisticated search is needed. We have found that a simulated annealing approach (see [32], Chapt. 10), provides a proper estimate of the time constants. In our realization we attributed $\log S(\vec{\gamma})$ to the "energy" and decreased the "temperature" of the simulated annealing from 0.1 to $5 \cdot 10^{-3}$, multiplying it at each step by 0.999999. The variations of the vector $\vec{\gamma}$ have been performed by adding at each step a random Gaussian vector with amplitude 0.05. To estimate the reliability of the procedure, we performed four runs, checking if the same values of the time constants $\vec{\gamma}$ and the same values of the coupling matrix C are reached in these independent implementations of the annealing. The results for a time series of length $M = 1000$ are shown in fig. 4. One can see that the reconstruction is not perfect, however, the likelihood that the relative error for the coupling constants that are larger than 0.1 is less than 10%.

Conclusions. – In summary, we have developed a method to reconstruct the connections of the network behind a collection of interacting neural fields, provided the observations of the potentials at the nodes are available. The method delivers the connectivity matrix, together with the parameters (time constants) characterizing the dynamics of the nodes, and the nonlinear gain functions defining the interactions. No prior knowledge on any of these parameters is required, only the general structure of the system is supposed to be known. We have assumed that data for all the nodes are available; the exploration of the situation with unobserved nodes is a subject of ongoing research.

Our method heavily relies on the diversity of the dynamics, and works most powerfully in the case the dynamics is chaotic. Additional tests have shown that even for a periodic dynamics, if this is complex enough (*i.e.*, the wave form is nontrivial with several minima and maxima over the period) to ensure sufficient diversity, the reconstruction works well. However, if the dynamics is periodic with a simple sine-type waveform, the reconstruction fails as the vectors used in the SVD analysis are not independent.

It is worth comparing our approach with other methods of dynamical network reconstruction. The most similar approach is that of ref. [33], where a neural network model in the firing rate formulation was considered. The difference to the present work is that in the firing rate formulation, instead of eqs. (1), one has a system

$$\frac{\mathrm{d}y_j}{\mathrm{d}t} + \gamma_j y_j = G_j\left(\sum_{k=1}^{n} C_{jk} y_k\right), \quad j = 1, \ldots, n\,. \qquad (6)$$

Because of the different order of applying a nonlinear function G and a linear coupling, to treat system (6) one has to invert the gain function G, instead of inverting the coupling matrix C. Therefore, the approach of ref. [33] applies to invertible gain functions only, while in the present case no restriction on the nonlinear functions in (1) is imposed —instead here the coupling matrix has to be non-singular, what appears to be a typical case for random matrices. In ref. [21] a general setup of high-dimensional dynamical systems coupled via a network of nonlinear interactions was considered. It was assumed that all nonlinear functions defining the local dynamics and the coupling are known, so the only unknown parameters, the coupling constants, could be reconstructed provided the full high-dimensional time series from all sites are available. Similar assumptions have been made in refs. [25,34,35]. In the present work, no knowledge on the nonlinear coupling functions is required. The local dynamics is assumed to be linear, thus only one unknown parameter (time constant) has to be determined at each node. In ref. [36] applications of compressive sensing methods to network reconstruction are reviewed. In these methods one assumes the network to be sparse, while no such assumption is needed for our approach.

* * *

We acknowledge useful discussions with M. Rosenblum and I. Sysoev. Results from the second and third

sections were supported by the Russian Science Foundation (Contract No. 17 12 01534).

REFERENCES

[1] Li Z., Li P., Krishnan A. and Liu J., *Bioinformatics*, **27** (2011) 2686.
[2] Sugihara G., May R., Ye H., Hsieh C.-h., Deyle E., Fogarty M. and Munch S., *Science*, **338** (2012) 496500.
[3] Oates C. J., Dondelinger F., Bayani N., Korkola J., Gray J. W. and Mukherjee S., *Bioinformatics*, **30** (2014) i468.
[4] Tomovski I. and Kocarev L., *Physica A: Stat. Mech. Appl.*, **436** (2015) 272.
[5] Trejo Banos D., Millar A. J. and Sanguinetti G., *Bioinformatics*, **31** (2015) 3617.
[6] Hirata Y., Amig'o J. M., Matsuzaka Y., Yokota R., Mushiake H. and Aihara K., *PLOS ONE*, **11** (2016) 1.
[7] Tirabassi G., Sommerlade L. and Masoller C., *Chaos*, **27** (2017) 035815.
[8] Volpe G., D'Ausilio A., Badino L., Camurri A. and Fadiga L., *Philos. Trans. R. Soc. B - Biol. Sci.*, **371** (2016) 20150377.
[9] Dickten H. and Lehnertz K., *Phys. Rev. E*, **90** (2014) 062706.
[10] Maksimow A., Silfverhuth M., Lngsj J., Kaskinoro K., Georgiadis S., Jskelinen S. and Scheinin H., *PLOS ONE*, **9** (2014) 1.
[11] Pastrana E., *Nat. Methods*, **10** (2013) 481.
[12] Sporns O., *Nat. Methods*, **10** (2013) 491.
[13] Boly M., Massimini M., Garrido M., Gosseries O., Noirhomme Q., Laureys S. and Soddu A., *Brain Connect.*, **2** (2012) 1.
[14] Lehnertz K., *Physiol. Meas.*, **32** (2011) 1715.
[15] Chicharro D., Andrzejak R. and Ledberg A., *BMC Neurosci.*, **12** (2011) P192.
[16] Yu D. and Parlitz U., *PLoS ONE*, **6** (2011) e24333.
[17] Lusch B., Maia P. D. and Kutz J. N., *Phys. Rev. E*, **94** (2016) 032220.
[18] Schelter B., Timmer J. and Eichler M., *J. Neurosci. Methods*, **179** (2009) 121.
[19] Andrzejak R. G. and Kreuz T., *EPL*, **96** (2011) 50012.
[20] Yang G., Wang L. and Wang X., *Sci. Rep.*, **7** (2017) 2991.
[21] Shandilya S. G. and Timme M., *New J. Phys.*, **13** (2011) 013004.
[22] Kralemann B., Pikovsky A. and Rosenblum M., *Chaos*, **21** (2011) 025104.
[23] Kralemann B., Pikovsky A. and Rosenblum M., *New J. Phys.*, **16** (2014) 085013.
[24] Sysoev I. V., Prokhorov M. D., Ponomarenko V. I. and Bezruchko B. P., *Phys. Rev. E*, **89** (2014) 062911.
[25] Levnajić Z. and Pikovsky A., *Sci. Rep.*, **4** (2014) 5030.
[26] Sysoev I. V., Ponomarenko V. I., Kulminskiy D. D. and Prokhorov M. D., *Phys. Rev. E*, **94** (2016) 052207.
[27] Hoppensteadt F. C. and Izhikevich E. M., *Weakly Connected Neural Networks* (Springer, Berlin) 1997.
[28] Bressloff P. C., *J. Phys. A: Math. Theor.*, **45** (2012) 033001.
[29] Ermentrout G. B. and Terman D. H., *Mathematical Foundations of Neuroscience Interdisciplinary Applied Mathematics*, Vol. **35** (Springer, New York) 2010, http://dx.doi.org/10.1007/978-0-387-87708-2.
[30] Sompolinsky H., Crisanti A. and Sommers H. J., *Phys. Rev. Lett.*, **61** (1988) 259.
[31] Trefethen L. N. and Bau III D., *Numerical Linear Algebra* (Society for Industrial and Applied Mathematics (SIAM), Philadelphia, PA) 1997.
[32] Press W. H., Flannery B. P., Teukolsky S. A. and Vetterling W. T., *Numerical Recipes* (Cambridge University Press, Cambridge) 1989.
[33] Pikovsky A., *Phys. Rev. E*, **93** (2016) 062313.
[34] Levnajic Z., *Eur. Phys. J. B*, **86** (2013) 298.
[35] Leguia M. G., Andrzejak R. G. and Levnajic Z., *J. Phys. A*, **50** (2017) 334001.
[36] Wang W.-X., Lai Y.-C. and Grebogi C., *Phys. Rep.*, **644** (2016) 1.